Maturation of Neuromuscular Transmission During Early Development in Zebrafish

PETER V. NGUYEN, LAURENT ANIKSZTEJN, STEFANO CATARSI, AND PIERRE DRAPEAU
Centre for Research in Neuroscience, McGill University and Montreal General Hospital Research Institute, Montreal, Quebec H3G 1A4, Canada

Nguyen, Peter V., Laurent Aniksztejn, Stefano Catarsi, and Pierre Drapeau. Maturation of neuromuscular transmission during early development in zebrafish. *J. Neurophysiol.* 81: 2852–2861, 1999. We have examined the rapid development of synaptic transmission at the neuromuscular junction (NMJ) in zebrafish embryos and larvae by patch-clamp recording of spontaneous miniature endplate currents (mEPCs) and single acetylcholine receptor (AChR) channels. Embryonic (24–36 h) mEPCs recorded in vivo were small in amplitude (<50 pA). The rate of mEPCs increased in larvae (3.5-fold increase measured by 6 days), and these mEPCs were mostly of larger amplitude (10-fold on average) with (≤5-fold) faster kinetics. Intracellular labeling with Lucifer yellow indicated extensive coupling between muscle cells in both embryos and larvae (≤10 days). Blocking acetylcholinesterase (AChE) with eserine had no effect on mEPC kinetics in embryos at 1 day and only partially slowed (by ~½) the decay rate in larvae at 6 days. In acutely dissociated muscle cells, we observed the same two types of AChR with conductances of 45 and 60 pS and with similar, brief (<0.5 ms) mean open times in both embryos and larvae. We conclude that AChR properties are set early during development at these early stages; functional maturation of the NMJ is only partly shaped by expression of AChE and may also depend on postsynaptic AChR clustering and presynaptic maturation.

INTRODUCTION

Understanding the mechanism of synapse formation during embryonic development is an important goal of neurobiology. Much of what we know about the formation and maturation of synapses is based on studies of the highly accessible peripheral neuromuscular junction (NMJ). The cellular and molecular events taking place during embryonic development of the NMJ have been characterized in considerable detail in vitro and in vivo in a variety of vertebrate and mammalian species (reviewed by Hall and Sanes 1993; Jacobson 1991). Ultimately, the cellular analysis of functional development needs to be determined in vivo. Detailed studies of neuromuscular synapse formation have been performed with cultured cells, but only a few studies have examined the functional changes occurring in vivo because of the difficulty of performing electrophysiological recordings in early embryos.

Early studies (before the advent of high-resolution patch-clamp techniques) reported developmental transitions in endplate potentials in the embryonic rat (Bennett and Pettigrew 1974; Dennis et al. 1981; Diamond and Miledi 1962) and *Xenopus* (Kullberg et al. 1977). We chose to investigate the development of neuromuscular transmission in the zebrafish for a variety of reasons. First, this animal offers the advantage of obtaining large numbers of externally fertilized eggs at precise developmental stages that are easily identified because of the optical clarity of the embryos. In particular, the migrations and pathfinding of identified neurons such as the spinal motoneurons have been described in detail in the embryo and larva (Myers et al. 1986; Westerfield et al. 1986) and appear to be related to the onset of early locomotor behaviors (Saint-Amant and Drapeau 1998). However, only limited physiological information is available concerning the development and properties of neuromuscular synaptic transmission (Grunwald et al. 1988; Liu and Westerfield 1988; Westerfield et al. 1986). In particular, an analysis of the endplate currents (EPCs) and the underlying single acetylcholine receptor (AChR) properties has not been done to date during in vivo NMJ maturation in any preparation. Another interest of the zebrafish is that recent genetic screens have identified mutations affecting embryonic locomotor behaviors (Granato et al. 1996), suggesting that the molecular bases of the development of these behaviors can be studied. However, an accurate description of the mutant phenotypes requires the characterization of the functional deficits before precise knowledge of the consequences of gene mutations can be established. A functional definition of embryonic locomotion requires an understanding of the mechanisms responsible for the maturation of motoneurons and of neuromuscular synaptic transmission, which together constitute "the final common pathway for all behavioral acts" (Sherrington 1947).

To examine the properties of developing neuromuscular synapses in the zebrafish, we have combined whole muscle cell patch-clamp recordings of synaptic activity in the embryo and larva in vivo and recordings of single AChRs in acutely dissociated muscle fibers at these two early developmental stages. By recording postsynaptic currents, we have been able to relate the properties of synaptic transmission to single AChR channels. Previous morphological studies have shown that the three primary motoneurons on either side of each of the segmented spinal cord somites extend axons that reach the muscle fibers along the middle of the segmental myotomes and form tiny "en passant" synapses starting at 17 h after fertilization (Liu and Westerfield 1992; Myers et al. 1986; Westerfield et al. 1986), which is the time at which spontaneous contractions of the tail are first observed (Saint-Amant and Drapeau 1998). These contractions eventually cease, and by 27 h the embryos swim briefly in response to a touch (Eaton and Farley 1973; Kimmel

The costs of publication of this article were defrayed in part by the payment of page charges. The article must therefore be hereby marked "*advertisement*" in accordance with 18 U.S.C. Section 1734 solely to indicate this fact.

et al. 1972; Saint-Amant and Drapeau 1998), the time at which the more numerous secondary motoneurons innervate the muscles (Myers et al. 1986; Westerfield et al. 1986). The embryos hatch on the second day of development, and within a few days the newborn larvae swim in short bursts at near-maximal rates (Eaton and Farley 1973; Kimmel et al. 1972; Saint-Amant and Drapeau 1998). We found it difficult to completely suppress (e.g., with TTX or high-Mg/low-Ca concentrations) the large-amplitude contractions, with the tail reaching the head of unrestrained embryos. It was thus not possible to maintain patch-clamp recordings from the very fragile (unfused) muscle cells in embryos <24 h old. We report here our observations with embryos between 24 and 30 h, when swimming is first manifested (Saint-Amant and Drapeau 1998), and contrast these with the observations in 3- to 6-day larvae, when swimming has reached a maximal rate. We show that the mEPCs increase greatly in frequency, amplitude, and kinetics during this early period of maturation without a change in AChR properties.

METHODS

Embryonic and larval zebrafish preparations

Whole cell voltage-clamp recordings of mEPCs were performed on living zebrafish embryos and larvae (ages 24 h to 6 days). All procedures were carried out in compliance with the guidelines stipulated by the Canadian Council for Animal Care and McGill University. Intact animals were anesthetized by immersion in tricaine (0.1 mg/ml, Sigma) dissolved in a modified extracellular saline solution (Westerfield et al. 1986) consisting of (in mM) 116 NaCl, 2 KCl, 0.7 $CaCl_2$, 10 $MgCl_2$, 10 glucose, and 10 HEPES, adjusted to pH 7.2, 290 mosmol. The reduced calcium and elevated magnesium concentrations were necessary to attenuate muscle contractions during our experiments. In some experiments, 1 μM TTX (Sigma) was added, and similar results were obtained. Fine tungsten wires (0.001 in.) were used to securely pin specimens through the notochord onto a Sylgard-lined petri dish. A glass needle and fine forceps were used to expose the axial muculature of a specimen by lifting and then carefully peeling its skin. After this initial procedure, tricaine was washed out and replaced with drug-free saline. The viability of the preparation was assessed by looking for vigorous heart contractions and blood circulation.

Whole cell voltage-clamp recordings

Standard whole cell voltage-clamp recordings (Hamill et al. 1981) were performed on dorsal and ventral muscle fibers (epaxial and hypaxial muscles) (see Myers 1985) in vivo under direct visualization with the use of Hoffmann modulation optics (×40 water immersion lens, Nikon Labophot microscope). All experiments were performed at room temperature (22°C). Patch-clamp electrodes were pulled from thin-walled, Kimax-51 borosilicate glass (3- to 5-MΩ resistance) and were filled with (in mM) 130 CsCl, 2 $MgCl_2$, 10 HEPES, 10 EGTA, and 4 NaATP, pH 7.2, 290 mosmol. The series resistance (5–10 MΩ) was compensated by 60–80%. Whole cell currents were recorded with an Axopatch-1D amplifier (Axon Instruments), filtered at 2 kHz (−3 dB) and digitized at 10 kHz, allowing the resolution of events with rise times of >0.1 ms. Data were acquired with pClamp 6.0 software (Axon Instruments) and were analyzed off-line with Axograph 3.5 (Axon Instruments). Cells with resting potentials less than −50 mV were discarded, and all recordings were obtained from a holding potential of −60 mV. For some experiments 0.1 mM eserine (Sigma), an inhibitor of acetylcholinesterase (AChE), was dissolved in the modified saline solution, and specimens were preincubated in drug for ≤30 min before recording to ensure penetration of the eserine. We performed statistical comparisons by using a Kolmogorov-Smirnov test for mEPC data.

Dye coupling

In some experiments fluorescent Lucifer yellow (Li salt; Sigma) was included (0.1%) in the patch pipette solution to determine the extent of coupling between the muscle cells at different developmental stages. In some experiments we added 1–3 mM halothane, 1-octanol, or 1-heptanol (Sigma) to the extracellular solution and superfused the preparations for ≤30 min before starting the recordings to uncouple the cells with these gap junction blockers. The cells were photographed with a still camera after removing the pipette at the end of the experiment.

Acute dissociation of muscle cells

To enhance recording of single AChRs, we acutely dissociated muscle cells by treating skinned embryos (as described previously) for 5–10 min with 0.1% collagenase (Type XII, Sigma Chemical) dissolved in normal extracellular solution (containing 1.3 mM $CaCl_2$ and 1 mM $MgCl_2$). The collagenase was washed off, and the cells were dissociated with a fine glass needle while incubating the tissue fragments in a modified recording solution that was nominally Mg- and Ca-free and that contained 2 mM EDTA. Dissociated cells were transferred to tissue culture dishes coated with polylysine (Sigma) to enhance cell adhesion and were kept in normal extracellular solution for ≤2 h. No obvious changes in cell morphology were noticed during these short time periods.

Single-channel recording

Electrodes of 5- to 10-MΩ resistance were coated with dental wax to ~50 μm of their tips, and the recording solution level was kept low to reduce capacitive noise (<0.3 pA RMS). The electrodes were filled with either recording solution containing 1.3 mM $CaCl_2$, 1 mM $MgCl_2$, and 0.4 μM ACh for cell-attached recordings or with KCl pipette solution (as for whole cell recordings, but containing KCl instead of CsCl) for recording in the outside-out configuration (Hamill et al. 1981). Recordings were filtered at 5 kHz (−3 dB) and digitized at 20 kHz. Data were stored to computer disk or digital tape and were analyzed off-line with pClamp 6 software (Axon Instruments). For some experiments, cells were continuously superfused with recording solution containing drugs (0.4 μM ACh, 10 μM D-tubocurarine; Sigma). The membrane potential of the muscle fibers was determined in the whole cell configuration and was used to correct the pipette potential applied during recordings.

RESULTS

Morphological features of embryonic and larval muscle fibers in vivo

As an initial step toward a physiological characterization of neuromuscular synaptic properties in living zebrafish embryos, we compared the morphological features of myotomes and muscle fibers in embryos and larvae at two different developmental stages. Between 24 and 30 h postfertilization, chevron-shaped myotomes (Fig. 1*A*) were clearly demarcated in the dorsal (*top*) and ventral regions of the zebrafish embryo. However, individual myocytes within each segmental myotome could not be clearly discerned at this stage. Ventral axial muscles were less prominent at this stage than were dorsal muscles. In sharp contrast larvae showed long, fused muscle fibers with discrete striations at 2-μm intervals (an isolated

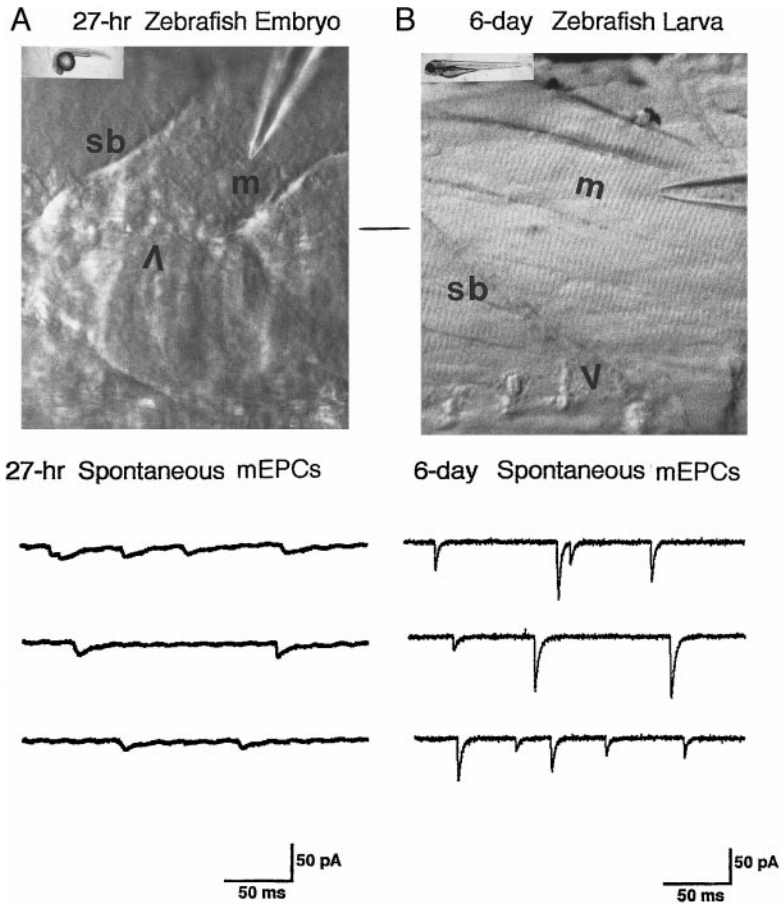

FIG. 1. Myotomal morphologies and miniature endplate currents (mEPCs) in a 27-h-old embryo (*A*) and a 6-day-old larva (*B*). sb: somite boundaries; arrowheads: ventral midline (out of focus in *A*); m: muscle cell. Unfused embryonic myocyte is seen between the m and the tip of the pipette in *A*, and a long, fused (polynucleated), striated muscle fiber is seen in the larva in *B*. mEPCs are small in size and slow in kinetics in the embryo (*A*) but have increased in amplitude and show faster kinetics in the larva (*B*). Whole cell voltage-clamp recordings were obtained at a holding potential of −60 mV in this and all subsequent mEPC recordings. Inset of each micrograph shows overall appearance of the zebrafish embryo and larva at these 2 developmental stages. In embryos, there is a large yolk sac situated just caudal to the head region. In these micrographs, dorsal is on top and rostral is to the left. Scale bar: 20 μm for muscle micrographs, 1 mm for insets.

muscle fiber from a 3-day larva is shown more clearly in Fig. 4A_2), and the demarcations between individual fibers were clearly evident (Fig. 1*B*). At this stage of development, skin peeling was easily performed, and the result was invariably a more pristine and intact preparation than with embryos.

Differential activity profiles in living embryos and larvae

We compared the spontaneous neuromuscular synaptic activity profiles of embryos (24–36 h) and larvae (3–6 days). We bathed the preparations in a high-Mg/low-Ca solution to prevent muscle contractions and to isolate spontaneous (presumably quantal) events. The recordings were performed near the middle of the somite, where neuromuscular innervation occurs (Liu and Westerfield 1992). Similar levels of synaptic activity were observed in preliminary experiments (not shown) in the presence of 1 μM TTX at a normal Ca concentration compared with the levels observed in high-Mg/low-Ca solution at both stages of development, indicating that these were spontaneous, not evoked, events. In embryos, whole cell voltage-clamp recordings of spontaneous miniature EPCs (mEPCs) revealed a mean frequency of 26 ± 20 (SD) min^{-1} ($n = 5$; Fig. 1*B* shows selected traces with several events each). In contrast, in 6-day larvae, the mean frequency was significantly higher, 92 ± 38 min^{-1} ($n = 5$; $P < 0.01$). Hence the mean frequency of spontaneous synaptic transmitter release was ~3.5-fold higher in the 6-day larvae than in the more immature 1-day embryos. The mEPCs were blocked at all stages in the presence of 10 μM D-tubocurarine, as shown previously for the block of neuromuscular transmission in larvae (Grunwald et al. 1988).

mEPCs recorded in embryos and larvae show distinct kinetic characteristics

A casual inspection of mEPCs recorded in embryos (Fig. 1*A*) and larvae (Fig. 1*B*) revealed two primary characteristics. First, mEPCs recorded from embryos were invariably small in size, in contrast to the larger mEPCs measured from larvae. Second, the embryonic mEPCs were slower in their kinetics of onset and decay than those observed in larvae. In general, mEPCs with fast kinetics of onset and decay emerged at ~36–42 h of development (not shown), and the transition from slow to fast mEPC kinetics was largely completed by 3 days of development.

A more thorough analysis of these mEPCs showed that in embryos the mean amplitude was 12.3 ± 10.4 pA ($n = 5$ muscle cells, in different animals). The amplitudes measured in larvae were significantly greater, 62.3 ± 16.1 pA at 3 days and 122.2 ± 120.7 pA at 6 days ($P < 0.005$, $n = 5$ preparations; Fig. 2, *A–E*, and Table 1). The median amplitudes at 27 h and 6 days were 7 and 73 pA, respectively (Fig. 2*F*). In no case could the amplitude histograms be described by a single Gaussian distribution. In summary, spontaneous mEPCs recorded at these two developmental stages differed significantly in their mean amplitudes.

We also observed significant age-dependent increases in the kinetics of onset and decay of mEPCs. The average mEPC rise times (10–90% maximum amplitude) in 24- to 36-h embryos versus 3- and 6-day larvae were 2.4 ± 2.1 ms versus 0.23 ± 0.04 ms and 0.49 ± 0.28 ms, respectively ($P < 0.0001$ for embryos compared with larvae, $n = 5$ for each age; Table 1).

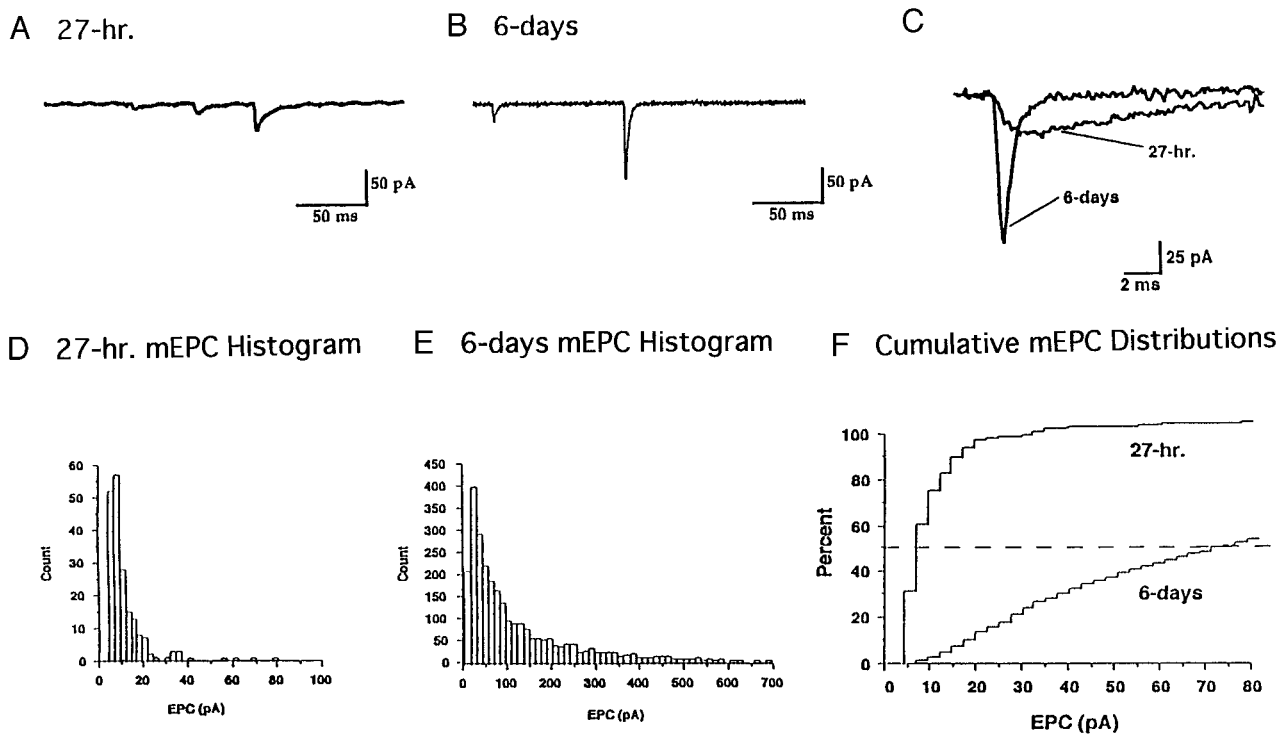

FIG. 2. mEPCs are smaller and slower in 27-h embryos (*A*) than in 6-day larvae (*B*). Sample traces (*C*) show clearly the more prolonged onset and decay kinetics in embryonic mEPCs compared with mEPCs obtained in a larva. Rise times (10–90%) of the traces obtained in embryos and larvae were 1.8 and 0.9 ms, respectively. Decay time constants for these traces were 6 ms for the embryonic mEPCs and 1.6 ms for the larval EPCs. *D*: histogram of mEPC amplitude distribution at 27 h. Most mEPCs were <50 pA in size. *E*: histogram of mEPC amplitude distribution at 6 days. Larger mEPCs were more evident in larvae than in embryos, resulting in a more skewed distribution. No single quantal distribution of amplitude peaks was evident at either stage of development. *F*: cumulative histogram of mEPC amplitudes measured in a 27-h embryo and a 6-day larva. Median mEPC sizes for embryos and larvae were 7 and 73 pA, respectively.

The medians of the rise time distributions for these two stages were 1.95 ms in embryos and 0.35 ms in 6 day larvae, respectively (Fig. 3*A*). In embryos, the mean decay time constant of mEPCs was 7.2 ± 2.3 ms (Table 1), which was significantly longer ($P < 0.0001$) than the mean decay time constant measured in larvae at 3 days (1.3 ± 0.4) and 6 days (2.1 ± 1.3 ms; Table 1). The median decay time constants for these two stages were 6.8 ms in embryos and 1.5 ms in 6-day larvae, respectively (Fig. 3*B*). Finally, there were clear biases in the distributions of mEPC sizes and their matching decay times at both stages (Fig. 3*C*). At 27 h, mEPCs were distributed such that the majority had decay time constants of >4 ms and amplitudes of <50 pA. In larvae by sharp contrast, mEPCs observed at 3 and 6 days had decay time constants that were mostly <2 ms, with relatively few events >4 ms in duration (Fig. 3*C*), and most of these mEPCs had amplitudes of >100 pA.

TABLE 1. *Summary of mEPC data*

Type of Recording	Mean mEPC Size, pA	Mean mEPC Rise Time, ms	Mean mEPC Decay Time Constant, ms
Whole cell, 27 h	12.3 ± 10.4	2.4 ± 2.1	7.2 ± 2.3
Whole cell, 3 day	62.3* ± 16.1	0.23* ± 0.04	1.3* ± 0.4
Whole cell, 6 day	122.2* ± 120.7	0.49* ± 0.28	2.1* ± 1.3

Values are means ± SD. For 27-h data: 420 events from 5 embryos; for 3-day data: 2,727 events from 5 larvae; for 6-day data: 2,650 events from 5 larvae. MEPC, miniature endplate current. * $P < 0.0001$, Kolmogorov-Smirnov test comparison with embryo data.

Coupling between muscle cells

One possible explanation for the presence of smaller and slower events in the embryonic muscle cells is if these are extensively coupled in the embryo and the coupling is lost at the larval stage, as described for *Xenopus* embryos (Armstrong et al. 1983) where the coupling is lost within 2 days of formation of the NMJ. Accordingly, the embryonic cells would be more affected by cable (or syncytial) filtering. We examined this by including the small, gap junction-permeable fluorescent dye Lucifer yellow in the patch pipette. As shown in Fig. 4, *B* and *D*, many other muscle cells were labeled with Lucifer yellow, indicating extensive coupling in both embryos (Fig. 4, *A* and *B*) and larvae (Fig. 4, *C* and *D*). Larval muscle cells remained coupled for ≤10 days, and only in older larvae (>14 days) did Lucifer yellow not pass into other cells (not shown), indicating a rather delayed uncoupling. However, the muscle fibers were too large at this stage for whole cell recordings of mEPCs.

In other experiments (not shown) we attempted to uncouple muscle cells in younger larvae and embryos by incubating these in the presence of 1–3 mM of the common gap junction uncouplers halothane, 1-octanol, or 1-heptanol (de Roos et al. 1996; Niggli et al. 1989). Halothane and 1-octanol failed to uncouple the cells; although 1-heptanol prevented coupling, it also eliminated mEPCs even at late stages (2–3 wk) when coupling was no longer present, suggesting a toxic effect, e.g., such as blockage of AChRs (Murrell et al. 1991). We were

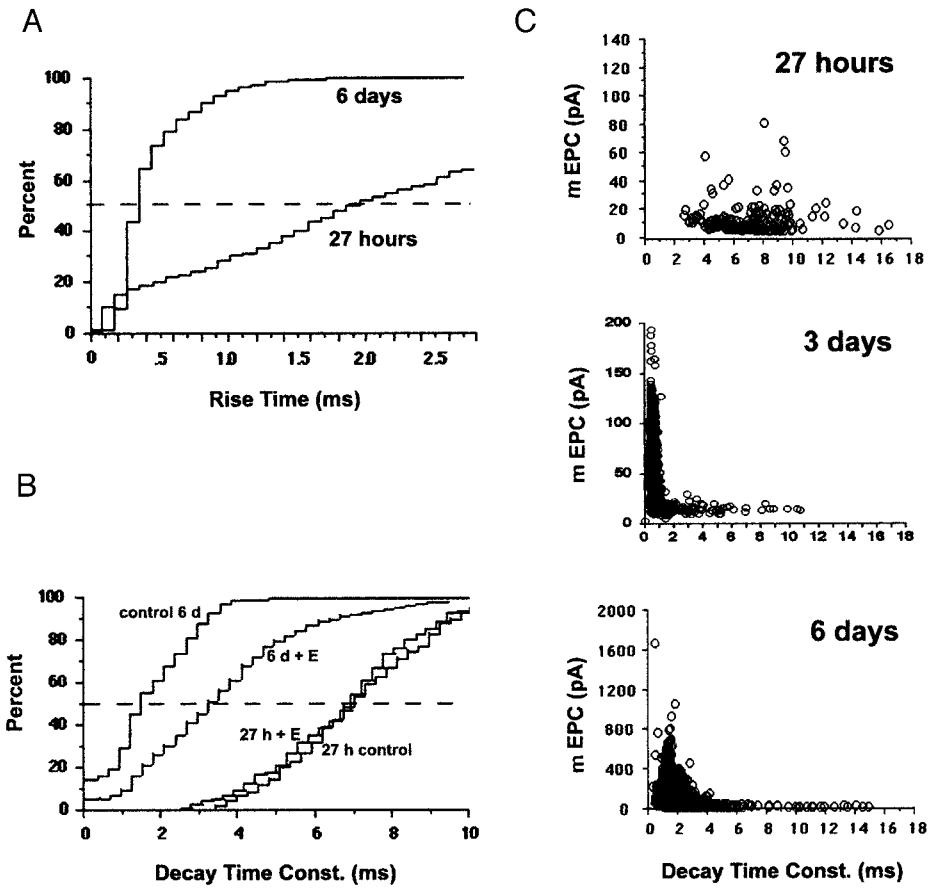

FIG. 3. mEPC kinetics in embryos and larvae. *A*: cumulative histogram of mEPC rise times. In 27-h embryos and 6-day larvae, mEPCs showed median rise times (10–90% maximum amplitudes) of 1.95 and 0.35 ms, respectively. *B*: cumulative histogram of mEPC decay time constants at 27 h showed longer decay times than at 6 days. Median times for these 2 stages were 6.8 and 1.5 ms, respectively. After acute treatment with eserine (0.1 mM), a cholinesterase inhibitor, the decay times in larvae were significantly prolonged, with a median decay time now shifted to 3.3 ms. Eserine had no significant effect on decay times of embryonic mEPCs. *C*: bivariate scattergrams of mEPC amplitudes and their corresponding decay time constants. Each point represents a single mEPC recorded in a 27-h embryo (*top*) and in larvae at 3 days (*middle*) or at 6 days (*bottom*). Most embryonic mEPCs are smaller than 50 pA and have decay times of >4 ms. In contrast, most larval mEPCs (at 3 and 6 days) are larger than 100 pA and have decay time constants of <1–2 ms.

therefore unable to directly test the effects of coupling on mEPC properties and conclude that extensive coupling exists at all the stages we could record from.

The small fraction (<5%) of low amplitude (<100 pA), slow (>4 ms) mEPCs observed in larvae (Fig. 3) could represent immature events similar to those observed in embryos or perhaps represent a minor population of poorly clamped events in the larger, larval muscle fibers, although we recorded from the middle of the fibers, presumably close to where they are innervated. That the mEPCs at 6 days were somewhat slower on average than at 3 days (Table 1) and had more of the very slow events (>4 ms) suggests that there was a small but gradual decrease in the effectiveness of the space clamp. This is consistent with an increase in muscle fiber size during this developmental period, and we were unable to effectively voltage clamp muscle cells in older larvae. We conclude that the mEPCs recorded in 24- to 27-h embryos were, on average, ~10-fold smaller in size and 3- to 4-fold slower in kinetics of onset and decay than were mEPCs measured in 6-day larvae.

Differential effects of AChE inhibition on mEPC decay times

What might be the molecular bases of the developmental difference in mEPC decay time constants? We addressed this question by first examining the effects of acute exposure of axial muscles to an inhibitor of AChE. We reasoned that blocking AChE, which hydrolyzes and inactivates the neuromuscular transmitter, should prolong the decay time constants of mEPCs because of decreased breakdown of and consequent prolonged exposure to ACh in the synaptic cleft. We found that, for embryos, 0.1 mM eserine had no significant effect on the mean decay time constant (6.0 ± 1.9 ms vs. 7.2 ± 2.3 ms in controls; $P > 0.2$, see Fig. 3*B* and Table 2). A similar lack of effect was observed at 1 mM eserine (not shown). However, we observed pronounced effects of eserine in larvae as mEPCs showed twofold longer decay time constants in the presence of the drug (Fig. 3*B* and Table 2). Nonetheless, it is noteworthy that the decay time constants measured in larvae in eserine (mean = 3.8 ms) did not match the embryonic control (drug-free) decay time constant (mean = 7.2 ms). Thus the activity of AChE in the synaptic cleft has only a partial role in determining the decay rates of mEPCs recorded in zebrafish axial muscles, and the transition from slow to fast mEPC decay rates cannot be attributed entirely to changes in AChE activity during development.

Similar AChR channels in embryonic and larval muscle cells

We hypothesized that the observed developmental alterations in mEPC kinetics may also arise from changes in the properties of AChR channels during development, such as the expression of different subunits or subtypes. To characterize the properties of AChRs, we recorded single-channel activity from acutely dissociated muscle cells. As shown in Fig. $5A_1$, myocytes from 1-day-old embryos were small, spherical cells of 10–20 μm in diameter. Muscle cells isolated from larvae were long, fused trapezoidal cells of 20–30 μm in diameter and ≤100 μm in length (Fig. $5A_2$). Regular striations were evident at 2-μm intervals. These dissociated cells thus appeared to retain the morphology observed in vivo (Fig. 1). We

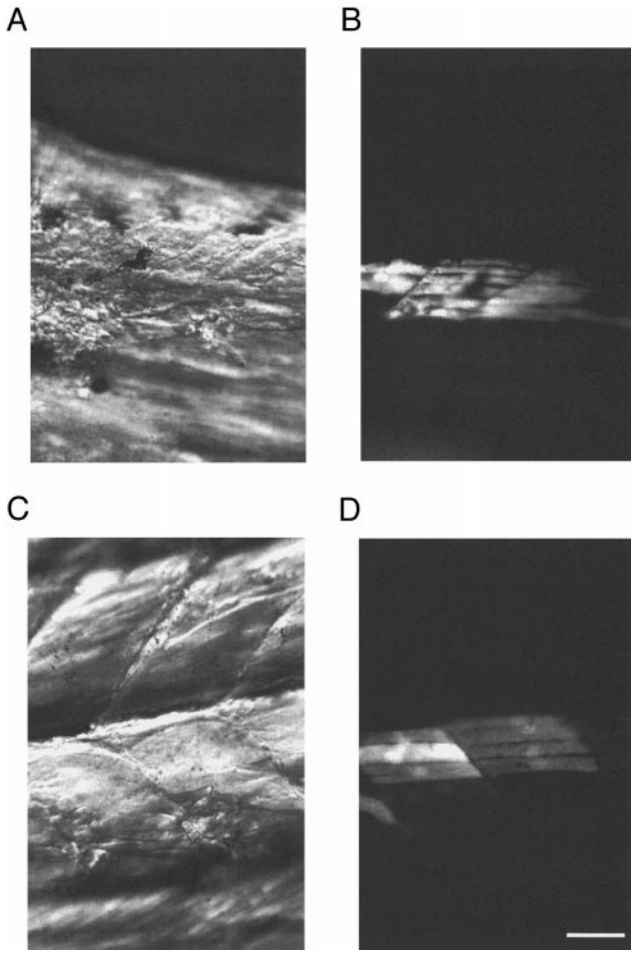

FIG. 4. Dye coupling among cells. Embryonic (29 h; *A* and *B*) and larval (4 day; *C* and *D*) muscle cells were filled with Lucifer yellow (*B* and *D*) dissolved in pipette solution during whole cell recording. Note that only the brightest cell was filled, whereas many other cells were coupled and labeled with Lucifer yellow.

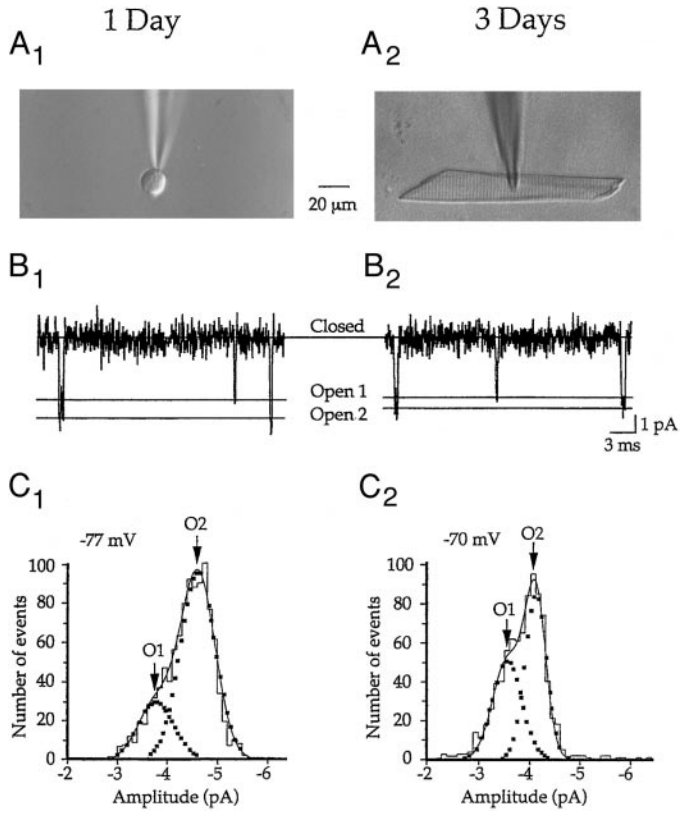

FIG. 5. Amplitudes of acetylcholine receptor (AChR) channel openings in muscle cells isolated from embryos and larvae. *A*: micrographs of muscle cells isolated from a 1-day embryo (A_1) and from a 3-day larva (A_2). Note the striations evident at 2-μm intervals in the larval muscle cell. *B*: sample recordings from cell-attached patches with 0.4 μM ACh in pipette, displaying openings to 2 different levels in an embryo (B_1, held at -77 mV) and a larva (B_1, held at -70 mV). *C*: amplitude histograms for the events recorded in *B* in an embryo (C_1) and a larva (C_2). Smooth lines are the combined Gaussian fits for 2 populations of events, indicated individually by the dotted curves. Peaks for the bottom amplitude events are denoted by arrows at O1 and the larger amplitude events at O2. Individual distributions are -3.8 ± 0.5 pA (O1 in C_1), -4.8 ± 0.5 pA (O2 in C_1), -3.5 ± 0.5 pA (O1 in C_2), and -4.1 ± 0.5 pA (O2 in C_2). Only 1 of each type of channel was present in the patches.

isolated muscle cells from 3-day-old larvae because cells from older specimens were more difficult to dissociate, and the developmental changes in mEPC properties were largely complete by this time. Unlike mammalian muscle fibers (Brehm and Kullberg 1987), there was no thickening of the en passant NMJ that could be discerned in early zebrafish muscle cells.

Cell-attached recordings with 0.4 μM ACh in the pipette from muscle cells at both embryonic and larval stages revealed two types of channels (Fig. 5, B_1 and B_2). Amplitude histograms of channel openings in the experiment illustrated in Fig. 5 were best fit by two Gaussian distributions (Fig. 5, C_1 and C_2) with predominantly larger amplitude events. On average the channels had slope conductances (Fig. 6*A*, estimated over a range of holding potentials) of 45 pS (45.3 $\pm$ 4.4 pS, $n = 28$) and 60 pS (60.1 $\pm$ 2.6 pS, $n = 27$) and mean open times of <1 ms, as described subsequently (based on all recordings presented in Table 3). These events were likely due to the presence of two distinct channels (rather than subconductance states) as patches containing one or the other type of channel were observed in approximately one-half (15/28) of the patches. Furthermore, when two channels were present, either one could predominate, although the 60-pS channel was seen more frequently. Occasionally other conductance levels were observed (usually of ~20, 35, and >100 pS), but unlike the 45- and 60-pS channels these proved to be insensitive to D-tubocurarine.

TABLE 2. *Effects of eserine on mean time constants of decay*

Experimental Condition	Mean Decay Time Constant, ms
27-h controls	7.2 $\pm$ 2.3 ($n = 5$, 420 events)
27-h + 0.1 mM eserine	6.0 $\pm$ 1.9 ($n = 5$, 247 events)
6-day controls	2.1 $\pm$ 1.3 ($n = 5$, 2650 events)
6-day + 0.1 mM eserine	3.8 $\pm$ 2.3* ($n = 6$, 1078 events)

Values are means $\pm$ SD. * $P < 0.0001$, Kolmogorov-Smirnov test comparison with controls. *n* is the number of recordings.

We characterized the properties of the channels in dissociated myocytes from embryos and larvae to ascertain whether their properties changed between these stages of development. As shown in Fig. 6*A*, ~45-pS and (more frequently) ~60-pS conductances were observed in embryonic myocytes and had reversal potentials near 0 mV. Similar conductances were observed in larval muscle cells as well (Table 3; Student's *t*-test, $P > 0.05$ for the difference between each type of

conductance in each "type of recording"). Single exponential distributions were normally observed for the open and closed time histograms (Fig. 6, B_1 and B_2) with means of <1 ms and of a few hundred milliseconds, respectively (Table 3). Only occasionally (4/55 channels analyzed) were second, longer open (~5 ms) or closed times (~400 ms) detected (as seen for a small number of events in Fig. 6, B_1, B_2, and C_1). Rather than reflecting distinct but rarely observed second states, we believe that these longer-lasting events were more likely due to missed events during unresolved bursts. We conclude that these channels shared similar kinetic properties in embryos and larvae despite their different conductances.

To ascertain that these were indeed AChR channels, the sensitivity of the channels to application of ACh (0.4 μM) and D-tubocurarine (10 μM) was examined in outside-out patches because synaptic currents were found to be abolished at this concentration of D-tubocurarine, which was shown previously to suppress neuromuscular transmission in the zebrafish (Grunwald et al. 1988). As shown in Fig. 7*A*, recordings from outside-out patches revealed channels with properties indistinguishable from those observed in cell-attached patches (Table 3) in that both 45- and 60-pS conductances with brief (<1 ms) openings were observed. A very low, spontaneous level of activity was observed in the absence of applied ACh (Control),

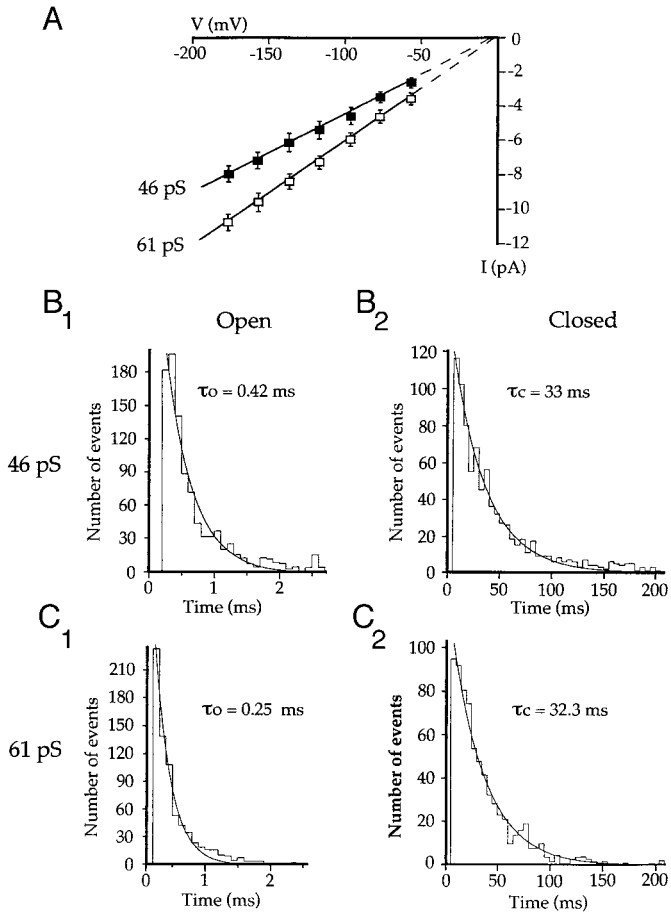

FIG. 6. Amplitude and dwell time distributions for 2 types of AChR channels recorded in an embryo. *A*: current-voltage relationship is plotted for events with slope conductances of 46 pS (■) and 61 pS (□) with extrapolated reversal potentials (- - -) near 0 mV. *B*: open (B_1) and closed (B_2) time distributions for 46-pS events. *C*: open (C_1) and closed (C_2) time distributions for 61-pS events. Mean times (from monoexponential fits) are indicated for each histogram.

TABLE 3. *Summary of AChR channel properties in zebrafish*

Type of Recording	Conductance, pS	Mean Open Time, ms	Mean Closed Time, ms
Cell attached			
24–36 h	46.1 ± 4.2 (9)	0.51 ± 0.17	111 ± 66
	60.5 ± 4.1 (12)	0.38 ± 0.15	74 ± 43
Cell attached			
3 days	46.1 ± 4.2 (9)	0.29 ± 0.14	83 ± 62
	58.7 ± 2.5 (7)	0.31 ± 0.10	241 ± 224
Outside out			
3 days	43.8 ± 4.8 (10)	0.26 ± 0.05	—
	60.1 ± 2.4 (8)	0.25 ± 0.05	543 ± 821

Values are means ± SD. Numbers in parentheses represent number of recordings. AChR, acetylcholine receptor.

and as shown in Fig. 7, *A* (ACh) and *B* (representative of 3 such experiments), the probability of channel opening increased rapidly on application of ACh. Channel activity was completely suppressed by subsequent application of 10 μM D-tubocurarine in the presence of ACh [Fig. 7, *A* (ACh + d-Tc) and *B*], confirming that these channels were indeed AChR channels. Furthermore, in 12 recordings from cell-attached patches with D-tubocurarine in the pipette solution, no channel activity was observed. We conclude from these results that the same two types of AChR are present throughout the developmental stages examined.

DISCUSSION

We have observed spontaneous mEPCs in zebrafish embryos between 24 and 36 h, with slow rise times of ~2 ms and decay times of ~7 ms. The mEPC amplitudes were 10–80 pA (mean 12 pA). Primary motoneurons start innervating the muscles at ~17 h postfertilization, the same time at which spontaneous tail contractions are first observed (Myers et al. 1986; Westerfield et al. 1986). This is also the earliest time at which clusters of AChRs have been detected in living embryos by staining with fluorescent α-bungarotoxin (Liu and Westerfield 1992). Thus AChR clustering appears to occur within a few hours of contact between the motoneurons and muscle cells. After hatching, when larvae are able to swim in fast bursts (Eaton and Farley 1973; Kimmel et al. 1972; Saint-Amant and Drapeau 1998), severalfold larger and faster synaptic currents were observed (rise times of <0.5 ms and decay times of <2 ms), suggesting an increased efficiency of transmission at maturing endplates. The neuronal sources of these mEPCs cannot be unambiguously defined because of polyneuronal innervation. The caudal primary motoneuron and numerous secondary motoneurons innervate the lateral ventral muscle fibers, whereas the middle primary motoneuron and secondary motoneurons innervate the dorsal muscles (Myers 1985; Westerfield et al. 1986). This polyneuronal innervation may account for the non-Gaussian distribution of mEPCs recorded at the stages we examined if different presynaptic endings activated synaptic responses of different amplitudes. Muscle cells were extensively coupled in both embryos and larvae for ≤2 wk, in contrast to the coupling between *Xenopus* embryonic muscle cells that is lost after ~2 days (Armstrong et al. 1983). This indicates that the trunk contractions during early larval swimming are mediated by a synsytium of coupled muscle fibers that may help minimize disparities in the extent

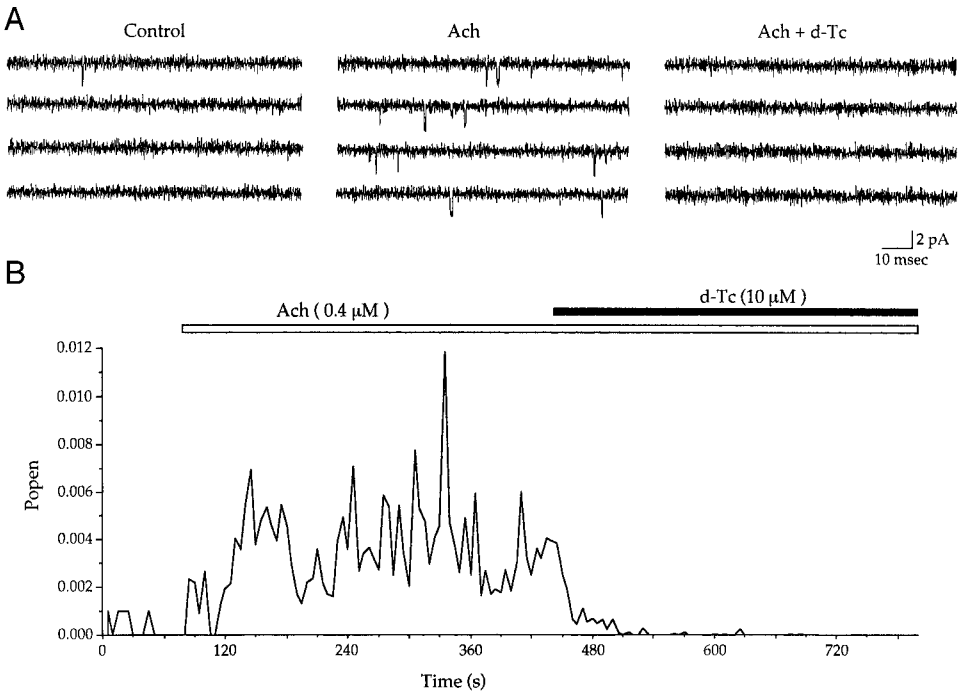

FIG. 7. ACh and D-tubocurarine (d-Tc) sensitivity of the AChR channels. *A*: sample traces from an outside-out patch isolated from 3-day larval muscle cell showing rare spontaneous openings before the addition of ACh (*left*, Control), a high rate of opening after addition of 0.4 μM ACh (*middle*), and the elimination of channel activity after addition of 10 μM d-Tc in the presence of 0.4 μM ACh (*right*). *B*: open probability plotted as a function of time course of the experiment. □: period during which the patch was exposed to 0.4 μM Ach; ■: application of 10 μM d-Tc.

of NMJ maturation by enhancing the overall performance of the muscle.

Two types of AChR channels were detected in muscle cells acutely dissociated from embryos, 45- and 60-pS conductance channels with mean open times of <1 ms. In the dissociated muscle cells, we could not distinguish between synaptic and extrasynaptic AChRs. However, in numerous other preparations, extrasynaptic AChRs appear to have properties similar to synaptically localized AChRs and provide direct information about the latter (Brehm and Kullberg 1987; reviewed by Edmonds et al. 1995; Schuetze and Role 1987). The same two types of AChR channels were observed in larvae, ruling out an obvious transition in channel properties during maturation at these early stages. However, more subtle changes, e.g., in modal gating of the channels (Naranjo and Brehm 1993) or in affinity for ACh, may not have been detected in our experiments. In many other preparations, a switch from slow- to fast-channel kinetics is observed during muscle maturation (reviewed by Jacobson 1991; Schuetze and Role 1987). A later postnatal switch in bovine (Mishina et al. 1986) and murine (Witzemann et al. 1996) AChR subunit composition has been shown to underlie the kinetic transitions in these species. Thus in most preparations it appears that postsynaptic events determine the early maturation of the NMJ during the first few days or weeks of development. In contrast, two types of AChR subtype with fast kinetics have also been observed in mice (Sheperd and Brehm 1997), and chick muscle has only one type of AChR with a mean open time that remains long (Schuetze 1980). Similar to these latter species, the AChR openings that we observed in zebrafish appear to remain constant (albeit brief) throughout the early developmental period that we examined, suggesting that the channel properties may be expressed from the onset of embryogenesis. As we did not examine the properties of mEPCs and AChRs in mature animals, we cannot exclude a later change in receptor properties. However it seems unlikely that the synaptic currents can get much faster than those in larvae as these are already among the fastest cholinergic responses to be reported and are close to the limit of detection (and effectiveness).

At the low concentration (0.4 μM) of ACh used here, only single AChR channel openings of <0.5 ms in duration were observed. At higher concentrations, bursts or clusters of openings have been observed in other preparations (reviewed by Edmonds et al. 1995; Lingle et al. 1992), and their durations appear to determine the time course of synaptic events (e.g., at *Xenopus* NMJs) (Kullberg and Owens 1986). Accordingly, we would expect several reopenings of AChRs at mature synapses, given the mean synaptic decay time constant of ~2 ms that we observed. It is interesting to note that in *Xenopus* (Kullberg and Owens 1986) and garter snakes (Dionne and Parsons 1978, 1981) the mEPC decay rates are related to contraction velocity. Because zebrafish larvae and adults show a high frequency (20–40 Hz) of contractions during swimming (Liu and Westerfield 1988; Saint-Amant and Drapeau 1998) and have faster and more pronounced startle contractions (Kimmel et al. 1972; Saint-Amant and Drapeau 1998), we propose that the physiological properties of the NMJ (brief AChR channel openings and fast mEPCs) have been optimized for these high rates of muscle contraction.

The immature synapses recorded in embryos had time constants of decay that were threefold longer than those recorded in larvae, suggesting prolonged channel reopenings during ACh release. The AChE inhibitor eserine caused only a twofold slowing of larval mEPCs and did not affect the time course of embryonic mEPCs, suggesting that AChE expression appears to be an important determinant for the maturation of synaptic transmission at NMJs but is not the only limit to mEPC decay. The limited contribution of AChE to shaping mEPCs may have contributed to the non-Gaussian amplitude histrograms observed both in embryos and larvae if the prolonged presence of ACh in the synaptic cleft produced broader and more variant patterns of AChR activation. AChR clusters increase in number and size early during

synaptogenesis (Liu and Westerfield 1992). Together with an increase in AChR density within clusters this could account for both the increase in mEPC amplitude and kinetics. Alternatively, presynaptic differentiation may determine the development of mature endplate properties in the zebrafish. It has been shown that the growth cones of *Xenopus* motoneurons in culture release ACh before contacting a muscle cell (Hume et al. 1983; Young and Poo 1983). Contact enhances the rate of release of ACh (Sun and Poo 1987; Xie and Poo 1986), and the kinetics and frequency of mEPCs increase with time in culture (Evers et al. 1989). These findings with cultured cells suggest that an extended diffusion barrier may exist at newly formed zebrafish NMJs in vivo and may result in delayed and prolonged activation of AChRs. Presynaptic contact with muscle cells could culminate in tight, restricted apposition of the motor nerve terminal to the muscle cell, and a higher density of AChE would accelerate the mEPC decay rate to that observed by 3 days. Regardless of the structural changes occurring during early development of the NMJ, our results indicate that the same AChRs are present in the embryo and larva and that AChE expression is not the only limit to maturation of the mEPC.

This work was supported by the following salary awards: a Medical Research Council Centennial Fellowship to P. V. Nguyen, a Fonds de la Recherche en Santé du Québec (FRSQ)-Institute National de la Santé et de la Recherche Médicale Visiting Fellow to L. Anikstejn, and an FRSQ Senior Research Scholarship to P. Drapeau. This work was also supported by a grant from the National Sciences and Engineering Research Council of Canada to P. Drapeau.

Present address: P. V. Nguyen, Dept. of Physiology and Division of Neurosciences, University of Alberta, Faculty of Medicine, Edmonton, Alberta T6G 2H7, Canada; L. Aniksztejn, INSERM U29, Hopital de Port-Royal, 123 Blvd. De Port Royal, 75014 Paris, France.

Address for reprint requests: P. Drapeau, Dept. of Neurology, Montreal General Hospital, 1650 Cedar Ave., Montreal, Quebec H3G 1A4, Canada.

Received 7 December 1998; accepted in final form 24 February 1999.

REFERENCES

ARMSTRONG, D. L., TURIN, L., AND WARNER, A. E. Muscle activity and the loss of electrical coupling between striated muscle cells in *Xenopus* embryos. *J. Neurosci.* 3: 1414–1421, 1983.

BENNETT, M. R. AND PETTIGREW, A. G. The formation of synapses in striated muscle during development. *J. Physiol. (Lond.)* 241: 515–545, 1974.

BREHM, P. AND KULLBERG, R. Acetylcholine receptor channels on adult mouse skeletal muscle are functionally identical in synaptic and non-synaptic membrane. *Proc. Natl. Acad. Sci. USA* 84: 2550–2554, 1987.

BUCHANAN, J., SUN, Y.-A., AND POO, M.-M. Studies of nerve-muscle interactions in *Xenopus* cell culture: fine structure of early functional contacts. *J. Neurosci.* 9: 1540–1554, 1989.

DENNIS, M. J., ZISKIND-CONHAIM, L., AND HARRIS, A. J. Development of neuromuscular junctions in rat embryos. *Dev. Biol.* 81: 266–279, 1981.

DE ROOS, A. D., VAN ZOELEN, E. J., AND THEUVENET, A. P. Determination of gap junctional intercellular communication by capacitance measurements. *Pflügers Arch.* 431: 556–563, 1996.

DIAMOND, J. AND MILEDI, R. A study of foetal and newborn rat muscle fibers. *J. Physiol. (Lond.)* 162: 393–408, 1962.

DIONNE, V. E. AND PARSONS, R. L. Synaptic channel gating differences at snake twitch and slow neuromuscular junctions. *Nature* 274: 902–904, 1978.

DIONNE, V. E. AND PARSONS, R. L. Characteristics of the acetylcholine-operated channel at twitch and slow fibre neuromuscular junctions of the garter snake. *J. Physiol. (Lond.)* 310: 145–158, 1981.

EATON, R. C. AND FARLEY, R. D. Development of the Mauthner neurons in embryos and larvae of the zebrafish, *Brachydanio rerio*. *Copeia* 4: 673–682, 1973.

EDMONDS, B., GIGG, A. J., AND COLQUHOUN, D. Mechanism of activation of muscle nicotinic acetylcholine receptors and the time course of the endplate currents. *Annu. Rev. Physiol.* 57: 469–493, 1995.

EVERS, J., LASER, M., SUN, Y.-A., XIE, Z.-P., AND POO, M.-M. Studies of nerve-muscle interactions in *Xenopus* cell culture: analysis of early synaptic currents. *J. Neurosci.* 9: 1523–1539, 1989.

FETCHO, J. R. Spinal network of the Mauthner cell. *Brain Behav. Evol.* 37: 298–316, 1991.

GRANATO, M., VAN EEDEN, F.J.M., SCHACH, U., TROWE, T., BRAND, M., FURUTANI-SEIKI, M., HAFFTER, P., HAMMERSCHMIDT, M., HEISENBERG, C.-P., JIANG, Y.-J., KANE, D. A., KELSH, R. N., MULLINS, M. C., ODENTHAL, J., AND NUSSLEIN-VOLHARD, C. Genes controlling and mediating locomotion behavior of the zebrafish embryo and larva. *Development* 123: 399–413, 1996.

GRUNWALD, D. J., KIMMEL, C. B., WESTERFIELD, M., WALKER, C., AND STREISIGNER, G. A neural degeneration mutant that spares primary neurons in the zebrafish. *Dev. Biol.* 126: 115–128, 1988.

HALL, Z. W. AND SANES, J. R. Synaptic structure and development: the neuromuscular junction. *Cell* 72/*Neuron* 10: 99–121, 1993.

HAMILL, O. P., MARTY, A., NEHER, E., SAKMANN, B., AND SIGWORTH, F. J. Improved patch-clamp techniques for high-resolution current recording from cells and cell-free membrane patches. *Pflügers Arch.* 391: 85–100, 1981.

HUME, R. I., ROLE, L. W., AND FISCHBACH, G. D. Acetylcholine release from growth cones detected with patches of acetylcholine receptor-rich membranes. *Nature* 305: 632–634, 1983.

JACOBSON, M. *Developmental Neurobiology* (3rd ed.). New York: Plenum, 1991.

KIMMEL, C. B., PATTERSON, J., AND KIMMEL, R. O. The development and behavioral characterisitcs of the startle response in the zebra fish. *Dev. Psychobiol.* 7: 47–60, 1972.

KULLBERG, R. AND OWENS, J. L. Comparative development of endplate currents in two muscles of *Xenopus laevis*. *J. Physiol. (Lond.)* 374: 413–427, 1986.

KULLBERG, R. W., LENTZ, T. L., AND COHEN, M. W. Development of the myotomal neuromuscular junction in *Xenopus laevis*: an electrophysiological and fine-structural study. *Dev. Biol.* 60: 101–129, 1977.

LINGLE, C. J., MACONOCHIE, D., AND STEINBACH, J. H. Activation of skeletal muscle nicotinic acetylcholine receptors. *J. Membr. Biol.* 126: 195–217, 1992.

LIU, D.W.C. AND WESTERFIELD, M. Function of identified motoneurons and co-ordination of primary and secondary motor systems during zebrafish swimming. *J. Physiol. (Lond.)* 403: 73–89, 1988.

LIU, D.W.C. AND WESTERFIELD, M. Clustering of acetylcholine receptors requires motoneurons in live embryos, but not in cell culture. *J. Neurosci.* 12: 1859–1866, 1992.

MISHINA, M., TAKAI, T., IMOTO, K., NODA, M., TAKAHASHI, T., NUMA, S., METHFESSEL, C., AND SAKMANN, B. Molecular distinction between fetal and adult forms of muscle acetylcholine receptor. *Nature* 321: 406–411, 1986.

MURRELL, R. D., BRAUN, M. S., AND HAYDON, D. A. Actions of n-alcohols on nicotinic acetylcholine receptor channels in cultured rat myotubes. *J. Physiol. (Lond.)* 437: 431–448, 1991.

MYERS, P. Z. Spinal motoneurons of the larval zebrafish. *J. Comp. Neurol.* 236: 555–561, 1985.

MYERS, P. Z., EISEN, J. S., AND WESTERFIELD, M. Development and axonal outgrowth of identified motoneurons in the zebrafish. *J. Neurosci.* 6: 2278–2289, 1986.

NARANJO, D. AND BREHM, P. Modal shifts in acetylcholine receptor channel gating confer subunit-dependent desensitization. *Science* 260: 1811–1814, 1993.

NIGGLI, E., RUDISULI, A., MAURER, P., AND WEINGART, R. Effects of general anesthetics on current flow across membranes in guinea pig myocytes. *Am. J. Physiol.* 256 (*Cell Physiol.* 25): C273–C281, 1989.

PIPERNO, G. AND FULLER, M. T. Monoclonal antibodies specific for an acetylated form of alpha-tubulin recognize the antigen in cilia and flagella from a variety of organisms. *J. Cell Biol.* 101: 2085–2094, 1985.

SAINT-AMANT, L. AND DRAPEAU, P. Time course of the development of motor behaviors in the zebrafish embryo. *J. Neurobiol.* 37: 622–632, 1998.

SCHUETZE, S. M. The acetylcholine channel open time in chick muscle is not decreased following innervation. *J. Physiol. (Lond.)* 303: 111–124, 1980.

SCHUETZE, S. M. AND ROLE, L. W. Developmental regulation of nicotinic acetylcholine receptors. *Annu. Rev. Neurosci.* 10: 403–457, 1987.

SHEPERD, D. AND BREHM, P. Two types of Ach receptors contribute to fast channel gating on mouse skeletal muscle. *J. Neurophysiol.* 78: 2966–2974, 1997.

SHERRINGTON, C. *The Integrative Action of the Nervous System* (2nd ed.). New Haven, CT: Yale Univ. Press, 1947.

SUN, Y.-A. AND POO, M.-M. Evoked release of acetylcholine from the growing embryonic neuron. *Proc. Natl. Acad. Sci. USA* 84: 2540–2544, 1987.

WESTERFIELD, M. *The Zebrafish Book*. Eugene, OR: Univ. of Oregon Press, 1993.

WESTERFIELD, M., MCMURRAY, J. V., AND EISEN, J. S. Identified motoneurons and their innervation of axial muscles in the zebrafish. *J. Neurosci.* 6: 2267–2277, 1986.

WITZEMANN, V., SCHWARTZ, H., KOENEN, M., BERBERICH, C., VILLAROEL, A., WERNIG, A., BRENNER, H. R., AND SAKMANN, B. Acetylcholine receptor E-subunit deletion causes muscle weakness and atrophy in juvenile and adult mice. *Proc. Natl. Acad. Sci. USA* 93: 13286–13291, 1996.

XIE, Z.-P. AND POO, M.-M. Initial events in the formation of neuromuscular synapse: rapid induction of acetylcholine release from embryonic neuron. *Proc. Natl. Acad. Sci. USA* 83: 7069–7073, 1986.

YOUNG, S. H. AND POO, M.-M. Spontaneous release of transmitter from growth cones of embryonic neurones. *Nature* 305: 634–637, 1983.